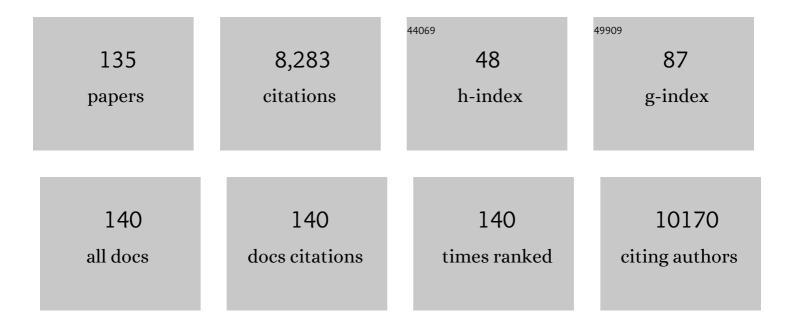
Hai-Feng Wang

List of Publications by Year in descending order

Source: https://exaly.com/author-pdf/5333562/publications.pdf Version: 2024-02-01



#	Article	IF	CITATIONS
1	Highly Ethylene‧elective Electrocatalytic CO ₂ Reduction Enabled by Isolated Cuâ^'S Motifs in Metal–Organic Framework Based Precatalysts. Angewandte Chemie, 2022, 134, .	2.0	5
2	Highly Ethylene‧elective Electrocatalytic CO ₂ Reduction Enabled by Isolated Cuâ^'S Motifs in Metal–Organic Framework Based Precatalysts. Angewandte Chemie - International Edition, 2022, 61, .	13.8	81
3	Selective methane electrosynthesis enabled by a hydrophobic carbon coated copper core–shell architecture. Energy and Environmental Science, 2022, 15, 234-243.	30.8	51
4	Structural rule of N-coordinated single-atom catalysts for electrochemical CO ₂ reduction. Journal of Materials Chemistry A, 2022, 10, 3585-3594.	10.3	13
5	Insight into the photoexcitation effect on the catalytic activation of H2 and C-H bonds on TiO2(110) surface. Chinese Chemical Letters, 2022, 33, 4705-4709.	9.0	9
6	A Universal Singleâ€Atom Coating Strategy Based on Tannic Acid Chemistry for Multifunctional Heterogeneous Catalysis. Angewandte Chemie, 2022, 134, .	2.0	9
7	A Universal Singleâ€Atom Coating Strategy Based on Tannic Acid Chemistry for Multifunctional Heterogeneous Catalysis. Angewandte Chemie - International Edition, 2022, 61, .	13.8	34
8	Constructing Structurally Ordered Highâ€Entropy Alloy Nanoparticles on Nitrogenâ€Rich Mesoporous Carbon Nanosheets for Highâ€Performance Oxygen Reduction. Advanced Materials, 2022, 34, e2110128.	21.0	44
9	Nanoscale hematoporphrin-based frameworks for photo-sono synergistic cancer therapy via utilizing Al(III) as metal nodes rather than heavy metals. Journal of Colloid and Interface Science, 2022, 616, 23-33.	9.4	16
10	Breaking through the Peak Height Limit of the Volcano-Shaped Activity Curve for Metal Catalysts: Role of Distinct Surface Structures on Transition Metal Oxides. Journal of Physical Chemistry C, 2022, 126, 183-191.	3.1	4
11	Optimally Selecting Photo- and Electrocatalysis to Facilitate CH ₄ Activation on TiO ₂ (110) Surface: Localized Photoexcitation versus Global Electric-Field Polarization. Jacs Au, 2022, 2, 188-196.	7.9	20
12	Modulating the Electronic Structure of FeCo Nanoparticles in Nâ€Đoped Mesoporous Carbon for Efficient Oxygen Reduction Reaction. Advanced Science, 2022, 9, e2200394.	11.2	52
13	Hydrogen Spillover-Bridged Volmer/Tafel Processes Enabling Ampere-Level Current Density Alkaline Hydrogen Evolution Reaction under Low Overpotential. Journal of the American Chemical Society, 2022, 144, 6028-6039.	13.7	179
14	In Operando Identification of In Situ Formed Metalloid Zinc ^{δ+} Active Sites for Highly Efficient Electrocatalyzed Carbon Dioxide Reduction. Angewandte Chemie - International Edition, 2022, 61, .	13.8	25
15	A Robust Hierarchical MXene/Ni/Aluminosilicate Glass Composite for Highâ€Performance Microwave Absorption. Advanced Science, 2022, 9, e2104163.	11.2	29
16	Universal Skeleton Feature of the Three-Dimensional Volcano Surface and the Thermodynamic Rule in Locating the Catalyst in Heterogeneous Catalysis. ACS Catalysis, 2022, 12, 247-258.	11.2	6
17	Achieving Theory–Experiment Parity for Activity and Selectivity in Heterogeneous Catalysis Using Microkinetic Modeling. Accounts of Chemical Research, 2022, 55, 1237-1248.	15.6	33
18	A Highly Efficient Nickel Phosphate Electrocatalyst for the Oxidation of 5-Hydroxymethylfurfural to 2,5-Furandicarboxylic Acid. ACS Sustainable Chemistry and Engineering, 2022, 10, 5538-5547.	6.7	12

#	Article	IF	CITATIONS
19	Partial Sulfidation Strategy to NiFeâ€LDH@FeNi ₂ S ₄ Heterostructure Enable Highâ€Performance Water/Seawater Oxidation. Advanced Functional Materials, 2022, 32, .	14.9	100
20	Oxygen vacancies and alkaline metal boost CeO2 catalyst for enhanced soot combustion activity: A first-principles evidence. Applied Catalysis B: Environmental, 2021, 281, 119468.	20.2	28
21	Towards the Circular Economy: Converting Aromatic Plastic Waste Back to Arenes over a Ru/Nb ₂ O ₅ Catalyst. Angewandte Chemie - International Edition, 2021, 60, 5527-5535.	13.8	169
22	<scp>CATKINAS</scp> : A largeâ€scale catalytic microkinetic analysis software for mechanism autoâ€analysis and catalyst screening. Journal of Computational Chemistry, 2021, 42, 379-391.	3.3	48
23	When Silicon Materials Meet Natural Sources: Opportunities and Challenges for Lowâ€Cost Lithium Storage. Small, 2021, 17, e1904508.	10.0	56
24	Mechanisms of Caromatic-C bonds cleavage in lignin over NbOx-supported Ru catalyst. Journal of Catalysis, 2021, 394, 94-103.	6.2	25
25	Pd single-atom monolithic catalyst: Functional 3D structure and unique chemical selectivity in hydrogenation reaction. Science China Materials, 2021, 64, 1919-1929.	6.3	75
26	Molecular Adsorption Kinetics: Nonlinear Entropy–Enthalpy Loss Quantified by Constrained AIMD and Insights into the Adsorption-Site Determination on Metal Oxides. Journal of Physical Chemistry C, 2021, 125, 10974-10982.	3.1	6
27	Origin of Water-Induced Deactivation of MnO ₂ -Based Catalyst for Room-Temperature NO Oxidation: A First-Principles Microkinetic Study. ACS Catalysis, 2021, 11, 6835-6845.	11.2	8
28	Revealing the boosting role of NO for soot combustion over CeO2(111): A first-principles microkinetic modeling. Molecular Catalysis, 2021, 509, 111582.	2.0	3
29	Cooperative Motion in Water–Methanol Clusters Controls the Reaction Rates of Heterogeneous Photocatalytic Reactions. Journal of the American Chemical Society, 2021, 143, 10940-10947.	13.7	12
30	Innenrücktitelbild: Boosting Photocatalytic Water Oxidation Over Bifunctional Rh ⁰ â€Rh ³⁺ Sites (Angew. Chem. 42/2021). Angewandte Chemie, 2021, 133, 23211-23211.	2.0	0
31	Boosting Photocatalytic Water Oxidation Over Bifunctional Rh 0 â€Rh 3+ Sites. Angewandte Chemie, 2021, 133, 22943.	2.0	2
32	Boosting Photocatalytic Water Oxidation Over Bifunctional Rh ⁰ â€Rh ³⁺ Sites. Angewandte Chemie - International Edition, 2021, 60, 22761-22768.	13.8	19
33	A Cationic Ru(II) Complex Intercalated into Zirconium Phosphate Layers Catalyzes Selective Hydrogenation via Heterolytic Hydrogen Activation. ChemCatChem, 2021, 13, 3801-3814.	3.7	7
34	Insight into the Surface-Tuned Activity and Cl ₂ /HCl Selectivity in the Catalytic Oxidation of Vinyl Chloride over Co ₃ O ₄ (110) versus (001): A DFT Study. Journal of Physical Chemistry C, 2021, 125, 16975-16983.	3.1	4
35	Understanding the Dynamic Potential Distribution at the Electrode Interface by Stochastic Collision Electrochemistry. Journal of the American Chemical Society, 2021, 143, 12428-12432.	13.7	24
36	Preparation and Characterization of High-Strength Glass-Ceramics via Ion-Exchange Method. Materials, 2021, 14, 5477.	2.9	4

#	Article	IF	CITATIONS
37	SSIA: A sensitivity-supervised interlock algorithm for high-performance microkinetic solving. Journal of Chemical Physics, 2021, 154, 024108.	3.0	17
38	Towards the object-oriented design of active hydrogen evolution catalysts on single-atom alloys. Chemical Science, 2021, 12, 10634-10642.	7.4	9
39	Resolving the Intricate Mechanism and Selectivity of Syngas Conversion on Reduced ZnCr ₂ O <i>_x</i> : A Quantitative Study from DFT and Microkinetic Simulations. ACS Catalysis, 2021, 11, 12977-12988.	11.2	24
40	Resolving the Two-Track Scaling Trend for Adsorbates on Rutile-Type Metal Oxides: New Descriptors for Adsorption Energies. Journal of Physical Chemistry C, 2021, 125, 23162-23168.	3.1	4
41	An effective structural descriptor to quantify the reactivity of lattice oxygen in CeO2 subnano-clusters. Physical Chemistry Chemical Physics, 2020, 22, 1721-1726.	2.8	12
42	Identifying the composition and atomic distribution of Pt-Au bimetallic nanoparticle with machine learning and genetic algorithm. Chinese Chemical Letters, 2020, 31, 890-896.	9.0	13
43	In situ NMR Investigation of the Photoresponse of Perovskite Crystal. Matter, 2020, 3, 2042-2054.	10.0	12
44	Direct Transformation of Glycerol to Propanal using Zirconium Phosphate‣upported Bimetallic Catalysts. ChemSusChem, 2020, 13, 4954-4966.	6.8	15
45	A novel heterogeneous Co(II)-Fenton-like catalyst for efficient photodegradation by visible light over extended pH. Science China Chemistry, 2020, 63, 1825-1836.	8.2	17
46	A general doping rule: rational design of Ir-doped catalysts for the oxygen evolution reaction. Chemical Communications, 2020, 56, 15201-15204.	4.1	9
47	Improved Performance of Nickel Boride by Phosphorus Doping as an Efficient Electrocatalyst for the Oxidation of 5-Hydroxymethylfurfural to 2,5-Furandicarboxylic Acid. Industrial & Engineering Chemistry Research, 2020, 59, 17348-17356.	3.7	42
48	The critical role of electrochemically activated adsorbates in neutral OER. Science China Materials, 2020, 63, 2509-2516.	6.3	16
49	Exploring dynamic interactions of single nanoparticles at interfaces for surface-confined electrochemical behavior and size measurement. Nature Communications, 2020, 11, 2307.	12.8	67
50	Heterogeneous Singleâ€Atom Catalysts for Electrochemical CO ₂ Reduction Reaction. Advanced Materials, 2020, 32, e2001848.	21.0	366
51	Synthesis of Cu2(OH)PO4 superstructures with NIR-laser enhanced photocatalytic activity. Functional Materials Letters, 2020, 13, 2050015.	1.2	1
52	Synthesis and Characterization of the CaTiO3:Eu3+ Red Phosphor by an Optimized Microwave-Assisted Sintering Process. Materials, 2020, 13, 874.	2.9	5
53	Flexible and Reusable Non-woven Fabric Photodetector Based on Polypyrrole/Crystal Violate Lactone for NIR Light Detection and Writing. Advanced Fiber Materials, 2020, 2, 150-160.	16.1	22
54	Amorphous Catalysis: Machine Learning Driven High-Throughput Screening of Superior Active Site for Hydrogen Evolution Reaction. Journal of Physical Chemistry C, 2020, 124, 10483-10494.	3.1	38

#	Article	IF	CITATIONS
55	Solvent Water Controls Photocatalytic Methanol Reforming. Journal of Physical Chemistry Letters, 2020, 11, 3738-3744.	4.6	11
56	A Simple Method To Locate the Optimal Adsorption Energy for the Best Catalysts Directly. ACS Catalysis, 2019, 9, 2633-2638.	11.2	24
57	Computational Simulation of Trapped Charge Carriers in TiO ₂ and Their Impacts on Photocatalytic Water Splitting. ACS Symposium Series, 2019, , 67-100.	0.5	1
58	Insight into room-temperature catalytic oxidation of NO by CrO2(110): A DFT study. Chinese Chemical Letters, 2019, 30, 618-623.	9.0	20
59	First principles study of Fenton reaction catalyzed by FeOCI: reaction mechanism and location of active site. Rare Metals, 2019, 38, 783-792.	7.1	14
60	Porphyrin sensitizers with modified indoline donors for dye-sensitized solar cells. Journal of Materials Chemistry C, 2018, 6, 3927-3936.	5.5	48
61	Theoretical insight into methanol steam reforming on indium oxide with different coordination environments. Science China Chemistry, 2018, 61, 336-343.	8.2	20
62	Identifying the key obstacle in photocatalytic oxygen evolution on rutile TiO2. Nature Catalysis, 2018, 1, 291-299.	34.4	212
63	Identifying Catalytically Active Mononuclear Peroxoniobate Anion of Ionic Liquids in the Epoxidation of Olefins. ACS Catalysis, 2018, 8, 4645-4659.	11.2	36
64	An efficient NixZryO catalyst for hydrogenation of bio-derived methyl levulinate to γ-valerolactone in water under low hydrogen pressure. Applied Catalysis B: Environmental, 2018, 227, 488-498.	20.2	40
65	Insight into Room-Temperature Catalytic Oxidation of Nitric oxide by Cr ₂ O ₃ : A DFT Study. ACS Catalysis, 2018, 8, 5415-5424.	11.2	32
66	Ce0.3Zr0.7O1.88N0.12 solid solution as a stable photocatalyst for visible light driven water splitting. Applied Catalysis B: Environmental, 2018, 224, 733-739.	20.2	4
67	First-Principles Insight into the Degradation Mechanism of CH ₃ NH ₃ Pbl ₃ Perovskite: Light-Induced Defect Formation and Water Dissociation. Journal of Physical Chemistry C, 2018, 122, 27340-27349.	3.1	28
68	Tuning Metal Catalyst with Metal–C ₃ N ₄ Interaction for Efficient CO ₂ Electroreduction. ACS Catalysis, 2018, 8, 11035-11041.	11.2	161
69	Activity Trend for Low-Concentration NO Oxidation at Room Temperature on Rutile-Type Metal Oxides. ACS Catalysis, 2018, 8, 10864-10870.	11.2	26
70	Insight into the Superior Catalytic Activity of MnO ₂ for Low-Content NO Oxidation at Room Temperature. Journal of Physical Chemistry C, 2018, 122, 25365-25373.	3.1	22
71	First-Principles Determination of CO Adsorption and Desorption on Pt(111) in the Free Energy Landscape. Journal of Physical Chemistry C, 2018, 122, 21478-21483.	3.1	29
72	Insights into the selective catalytic reduction of NO by NH3 over Mn3O4(110): a DFT study coupled with microkinetic analysis. Science China Chemistry, 2018, 61, 457-467.	8.2	26

#	Article	lF	CITATIONS
73	Insight into the NH ₃ -Assisted Selective Catalytic Reduction of NO on β-MnO ₂ (110): Reaction Mechanism, Activity Descriptor, and Evolution from a Pristine State to a Steady State. ACS Catalysis, 2018, 8, 9269-9279.	11.2	76
74	Alkali-assisted mild aqueous exfoliation for single-layered and structure-preserved graphitic carbon nitride nanosheets. Journal of Colloid and Interface Science, 2017, 495, 19-26.	9.4	37
75	Identifying the Role of Photogenerated Holes in Photocatalytic Methanol Dissociation on Rutile TiO ₂ (110). ACS Catalysis, 2017, 7, 2374-2380.	11.2	76
76	Cosensitized Porphyrin System for High-Performance Solar Cells with TOF-SIMS Analysis. ACS Applied Materials & Interfaces, 2017, 9, 16081-16090.	8.0	11
77	Understanding the Dual Active Sites of the FeO/Pt(111) Interface and Reaction Kinetics: Density Functional Theory Study on Methanol Oxidation to Formaldehyde. ACS Catalysis, 2017, 7, 4281-4290.	11.2	50
78	Crystal Structural Effect of AuCu Alloy Nanoparticles on Catalytic CO Oxidation. Journal of the American Chemical Society, 2017, 139, 8846-8854.	13.7	181
79	Tracking motion trajectories of individual nanoparticles using time-resolved current traces. Chemical Science, 2017, 8, 1854-1861.	7.4	127
80	Perspective: Photocatalytic reduction of CO2 to solar fuels over semiconductors. Journal of Chemical Physics, 2017, 147, 030901.	3.0	76
81	Significant enhancement of the selectivity of propylene epoxidation for propylene oxide: a molecular oxygen mechanism. Physical Chemistry Chemical Physics, 2017, 19, 25129-25139.	2.8	31
82	Unique Trapped Dimer State of the Photogenerated Hole in Hybrid Orthorhombic CH ₃ NH ₃ PbI ₃ Perovskite: Identification, Origin, and Implications. Nano Letters, 2017, 17, 7724-7730.	9.1	19
83	Theory and applications of surface microâ€kinetics in the rational design of catalysts using density functional theory calculations. Wiley Interdisciplinary Reviews: Computational Molecular Science, 2017, 7, e1321.	14.6	35
84	Unexpected C–C Bond Cleavage Mechanism in Ethylene Combustion at Low Temperature: Origin and Implications. ACS Catalysis, 2016, 6, 5393-5398.	11.2	27
85	Theoretical insights into how the first C–C bond forms in the methanol-to-olefin process catalysed by HSAPO-34. Physical Chemistry Chemical Physics, 2016, 18, 14495-14502.	2.8	21
86	Highly Efficient Epoxidation of Allylic Alcohols with Hydrogen Peroxide Catalyzed by Peroxoniobate-Based Ionic Liquids. ACS Catalysis, 2016, 6, 3354-3364.	11.2	35
87	Theoretical Study of Heteroatom Doping in Tuning the Catalytic Activity of Graphene for Triiodide Reduction. ACS Catalysis, 2016, 6, 6804-6813.	11.2	35
88	Reversibility Iteration Method for Understanding Reaction Networks and for Solving Microkinetics in Heterogeneous Catalysis. ACS Catalysis, 2016, 6, 7078-7087.	11.2	64
89	Direct hydrodeoxygenation of raw woody biomass into liquid alkanes. Nature Communications, 2016, 7, 11162.	12.8	359
90	Understanding Catalytic Reactions over Zeolites: A Density Functional Theory Study of Selective Catalytic Reduction of NO _{<i>x</i>} by NH ₃ over Cu-SAPO-34. ACS Catalysis, 2016, 6, 7882-7891.	11.2	99

#	Article	IF	CITATIONS
91	Revealing the Volcano-Shaped Activity Trend of Triiodide Reduction Reaction: A DFT Study Coupled with Microkinetic Analysis. ACS Catalysis, 2016, 6, 733-741.	11.2	41
92	Batteries: 2D Monolayer MoS ₂ –Carbon Interoverlapped Superstructure: Engineering Ideal Atomic Interface for Lithium Ion Storage (Adv. Mater. 24/2015). Advanced Materials, 2015, 27, 3582-3582.	21.0	6
93	Orange Zinc Germanate with Metallic GeGe Bonds as a Chromophoreâ€Like Center for Visibleâ€Lightâ€Driven Water Splitting. Angewandte Chemie - International Edition, 2015, 54, 11467-11471.	13.8	18
94	2D Monolayer MoS ₂ –Carbon Interoverlapped Superstructure: Engineering Ideal Atomic Interface for Lithium Ion Storage. Advanced Materials, 2015, 27, 3687-3695.	21.0	504
95	The search for efficient electrocatalysts as counter electrode materials for dye-sensitized solar cells: mechanistic study, material screening and experimental validation. NPG Asia Materials, 2015, 7, e226-e226.	7.9	52
96	The effects of the presence of metal Fe in the CO oxidation over Ir/FeOx catalyst. Catalysis Communications, 2015, 61, 83-87.	3.3	10
97	Theoretical investigation of NH ₃ â€SCR processes over zeolites: A review. International Journal of Quantum Chemistry, 2015, 115, 618-630.	2.0	26
98	Critical roles of co-catalysts for molecular hydrogen formation in photocatalysis. Journal of Catalysis, 2015, 330, 120-128.	6.2	59
99	Possibility of designing catalysts beyond the traditional volcano curve: a theoretical framework for multi-phase surfaces. Chemical Science, 2015, 6, 5703-5711.	7.4	40
100	Thermal behavior of cellulose diacetate melt using ionic liquids as plasticizers. RSC Advances, 2015, 5, 901-907.	3.6	21
101	Local atomic structure modulations activate metal oxide as electrocatalyst for hydrogen evolution in acidic water. Nature Communications, 2015, 6, 8064.	12.8	270
102	Catalyst screening: Refinement of the origin of the volcano curve and its implication in heterogeneous catalysis. Chinese Journal of Catalysis, 2015, 36, 1596-1605.	14.0	61
103	Identifying the distinct features of geometric structures for hole trapping to generate radicals on rutile TiO ₂ (110) in photooxidation using density functional theory calculations with hybrid functional. Physical Chemistry Chemical Physics, 2015, 17, 1549-1555.	2.8	61
104	Stable Isolated Metal Atoms as Active Sites for Photocatalytic Hydrogen Evolution. Chemistry - A European Journal, 2014, 20, 2088-2088.	3.3	3
105	Solar Cells: Highly Electrocatalytic Activity of RuO2Nanocrystals for Triiodide Reduction in Dye-Sensitized Solar Cells (Small 3/2014). Small, 2014, 10, 483-483.	10.0	3
106	Stable Isolated Metal Atoms as Active Sites for Photocatalytic Hydrogen Evolution. Chemistry - A European Journal, 2014, 20, 2138-2144.	3.3	173
107	A {0001} faceted single crystal NiS nanosheet electrocatalyst for dye-sensitised solar cells: sulfur-vacancy induced electrocatalytic activity. Chemical Communications, 2014, 50, 5569.	4.1	60
108	The effects of the Pd chemical state on the activity of Pd/Al ₂ O ₃ catalysts in CO oxidation. Catalysis Science and Technology, 2014, 4, 3973-3980.	4.1	73

#	Article	IF	CITATIONS
109	Highly Electrocatalytic Activity of RuO ₂ Nanocrystals for Triiodide Reduction in Dye‧ensitized Solar Cells. Small, 2014, 10, 484-492.	10.0	68
110	Selective Deposition of Ag ₃ PO ₄ on Monoclinic BiVO ₄ (040) for Highly Efficient Photocatalysis. Small, 2013, 9, 3951-3956.	10.0	215
111	Surface hydrogen bonding can enhance photocatalytic H2 evolution efficiency. Journal of Materials Chemistry A, 2013, 1, 14089.	10.3	113
112	Unidirectional suppression of hydrogen oxidation on oxidized platinum clusters. Nature Communications, 2013, 4, 2500.	12.8	197
113	Evidence To Challenge the Universality of the Horiuti–Polanyi Mechanism for Hydrogenation in Heterogeneous Catalysis: Origin and Trend of the Preference of a Non-Horiuti–Polanyi Mechanism. Journal of the American Chemical Society, 2013, 135, 15244-15250.	13.7	101
114	Active sites on hydrogen evolution photocatalyst. Journal of Materials Chemistry A, 2013, 1, 15258.	10.3	96
115	Rational screening low-cost counter electrodes for dye-sensitized solar cells. Nature Communications, 2013, 4, 1583.	12.8	365
116	Facet-Dependent Catalytic Activity of Platinum Nanocrystals for Triiodide Reduction in Dye-Sensitized Solar Cells. Scientific Reports, 2013, 3, 1836.	3.3	146
117	Turning Indium Oxide into a Superior Electrocatalyst: Deterministic Heteroatoms. Scientific Reports, 2013, 3, 3109.	3.3	28
118	Oxygen vacancy formation in CeO2 and Ce1â^'xZrxO2 solid solutions: electron localization, electrostatic potential and structural relaxation. Physical Chemistry Chemical Physics, 2012, 14, 16521.	2.8	80
119	Origin of extraordinarily high catalytic activity of Co3O4 and its morphological chemistry for CO oxidation at low temperature. Journal of Catalysis, 2012, 296, 110-119.	6.2	179
120	Ceria Foam with Atomically Thin Single rystal Walls. Angewandte Chemie - International Edition, 2012, 51, 3611-3615.	13.8	18
121	Structural Origin: Water Deactivates Metal Oxides to CO Oxidation and Promotes Lowâ€Temperature CO Oxidation with Metals. Angewandte Chemie - International Edition, 2012, 51, 6657-6661.	13.8	119
122	Exchange between sub-surface and surface oxygen vacancies on CeO2(111): a new surface diffusion mechanism. Chemical Communications, 2011, 47, 6105.	4.1	58
123	Direct catalytic conversion of furfural to 1,5-pentanediol by hydrogenolysis of the furan ring under mild conditions over Pt/Co2AlO4 catalyst. Chemical Communications, 2011, 47, 3924.	4.1	187
124	New insight into mechanisms in water-gas-shift reaction on Au/CeO2(111): A density functional theory and kinetic study. Faraday Discussions, 2011, 152, 121.	3.2	85
125	An understanding and implications of the coverage of surface free sites in heterogeneous catalysis. Journal of Chemical Physics, 2009, 130, 224701.	3.0	21
126	Maximizing the Localized Relaxation: The Origin of the Outstanding Oxygen Storage Capacity of κ e ₂ Zr ₂ O ₈ . Angewandte Chemie - International Edition, 2009, 48, 8289-8292.	13.8	85

#	Article	IF	CITATIONS
127	Structure and Catalytic Activity of Gold in Low-Temperature CO Oxidation. Journal of Physical Chemistry C, 2009, 113, 6124-6131.	3.1	32
128	NO Oxidation on Platinum Group Metals Oxides: First Principles Calculations Combined with Microkinetic Analysis. Journal of Physical Chemistry C, 2009, 113, 18746-18752.	3.1	56
129	xmlns:mml="http://www.w3.org/1998/Math/MathML" display="inline"> <mml:mrow><mml:mn>4f</mml:mn></mml:mrow> electrons on defective <mml:math <br="" xmlns:mml="http://www.w3.org/1998/Math/MathML">display="inline"><mml:mrow><mml:msub><mml:mrow><mml:mtext>CeO</mml:mtext></mml:mrow><mml:mn></mml:mn></mml:msub></mml:mrow></mml:math>	3.2 2 <td>233 1n> </td>	233 1n>
130	Origin and impl. Physical Review B, 2009, 79, . A Model to Understand the Oxygen Vacancy Formation in Zr-Doped CeO ₂ : Electrostatic Interaction and Structural Relaxation. Journal of Physical Chemistry C, 2009, 113, 10229-10232.	3.1	113
131	Au on (111) and (110) surfaces of CeO2: A density-functional theory study. Surface Science, 2008, 602, 1736-1741.	1.9	95
132	Examining the redox and formate mechanisms for water–gas shift reaction on Au/CeO2 using density functional theory. Surface Science, 2008, 602, 2828-2834.	1.9	76
133	Gold Segregation Improves Electrocatalytic Activity of Icosahedron Au@Pt Nanocluster: Insights from Machine Learning â€. Chinese Journal of Chemistry, 0, , .	4.9	10
134	Operando Metalloid Znδ+ Active Sites for Highly Efficient Carbon Dioxide Reduction Electrocatalysis. Angewandte Chemie, 0, , .	2.0	0
135	Oriented design of triple atom catalysts for electrocatalytic nitrogen reduction with the genetic-algorithm-based global optimization method driven by first principles calculations. Journal of Materials Chemistry A, 0, , .	10.3	5